In-Orbit Modelling and Calibration of the Sun Sensors

On UoSAT-12 and Tsinghua-1 Satellites

Shu-Fan Wu and Willem H. Steyn

Surrey Space Centre
University of Surrey
Guildford, Surrey, GU2 7XH, United Kingdom
Fax: +44 1483 259503, Tel: +44 1483 259278
Emial: Shufan.Wu@surrey.ac.uk, H.Steyn@surrey.ac.uk

Abstract: The modelling relations and calibration techniques of the miniature analogue sun sensors, developed at Surrey Satellite Technology Limited (SSTL), are discussed in this paper. Two model equations, an algebraic model based on a multi-variable polynomial algebraic curve-fitting procedure and a physical model based on analytical geometry relations, were developed. Parameter sensitivity analyses were conducted for the physical model, and an in-orbit calibration approach is proposed and was implemented with the sun sensors on-board UoSAT-12 and Tsinghua-1. A sequential batch filter algorithm was developed, based on the principle of the least-square estimation for regression models, to handle the large amount of in-orbit data in a sequential way. Satisfactory performance improvements have been achieved through the in-orbit calibration analyses for both satellites.

1. Introduction

Among optoelectronic devices for attitude determination and control of space vehicles, the devices for sun attitude determination (sun sensors) excel in small mass, large field of view, low cost and power consumption, and are less computational demanding and susceptible to interference in practice[1-2]. The main disadvantage is that these sensors cannot be used during the orbit eclipse phase. However, this restriction is not so critical in many application cases, where alternative sensors, such as earth horizon sensors, magnetometers, star sensors, are available for attitude determination to a lower or higher accuracy. Therefore, sun sensors are the most widely used sensor type in various space missions[1-4]. Recent development in micro electro-mechanical systems technology has led to the development of low cost, low power, miniature sun sensors, which are ideal for use on small spacecraft, such as mini/micro/nano-satellites.

The miniature analogue 2-axis sun sensor, developed at Surrey Satellite Technology Limited (SSTL), is a low-cost attitude determination sensor suitable for a wide range of space missions. It measures the sun angle in two orthogonal axes. A custom-made solar cell detector and a small slit mask are used for each measurement axis. Specially designed electronic circuits are mounted inside the sensor to pick up the signals from the solar cell detector, to amplify and filter out noise, and to produce clean and reliable output signals. The output from each sensor axis consists of 3 analogue 0-5 Volt signals which are used to determine the relevant sun angles, through an appropriate processing algorithm implemented in the on-board computer (OBC) of the satellite. Table 1 summarizes the sun sensor's major performance specifications and physical characteristics. Figure 1 shos a photograph of the sun sensor unit.

Figure 1 A sun sensor unit

1

**Table 1** Performance of the SSTL 2-Axis Sun Sensor

Speciofication	Performance
Measuring Axes:	2 orthogonal axes
Measuring Field of View:	+/- 50 °
Measuring Accuracy:	0.5 ° (3σ)
Output Signals	6×5 V : channels
Power Supply:	+/- 12V
Physical Dimensions:	95×107×35 mm
Physical Mass:	0.3 kg
Operation Temp:	-50ºC to +80ºC
Power Consumption:	Sunlit: <100mW; Dark: <1mW

The major technical problem in the sun sensor's development and application is how to relate the output signals with the relevant sun angles to a good accuracy, that is, how to model the relationship between the angles to be measured and the sensor's output signals. What makes the modelling more complicated and difficult is that there is also a cross-coupling effect between the two orthogonal axes measurements. Although it is very small, the coupling effect will limit the sensor's accuracy if not properly modelled and calibrated. Furthermore, the measuring accuracy is also affected by the final installation alignment to the spacecraft, influenced by the launch, and the space environments. These kinds of influences cannot be compensated for during ground calibration tests, which means an in-orbit calibration should be applied further to increase the measurement accuracy.

This paper is aiming to develop the model equations, to investigate the coupling relation between two axes, and further to explore the in-orbit calibration techniques when the sensor is in operation once in space. The paper is organised as follows. Section 2 describes the sensor principle of working and the ground test scheme for modelling and analyses. Section 3 discusses a multi-variable algebraic curve-fitting approach, where a high-order polynomial function is used to describe the calibration model. Section 4 presents a physical modelling approach, where an analytical model equation is set up from the sensor's physical and geometrical relations. Sensitivity analysis for each model parameter is also conducted aiming for a better understanding of the model relation. Section 5 describes an in-orbit calibration scheme based on the tangent-based physical model relation, which has been evaluated through practical experiments with the sun sensors on-board UoSAT-12 and Tsinghua-1 satellites. Finally some conclusions are summarized in Section 6.

2. Operation Principle and Test Experiments

The operation principle of the sun sensor is mainly based on the double triangle detector module made from custom-made solar cell material. It consists of a monolithic pair of triangle silicon detectors mounted in an aluminium housing. A quartz window is placed above the silicon detector, which has a photomasked aperture (slit) casting a line image of the sunlight across the two adjacend triangles. The basic operating principle is shown in Fig.2, where the monolithic pair of triangle silicon detectors are placed side by side, referred to as A and B. The bold line drawn across the detectors represents the sunlight's image as casted through the long aperture. This suns image stimulate the corresponding detector cells, which produce electrical signals proportional to the length of the line image on each triangle. Assign A and B to represent the two signals produced from the two triangular detectors respectively, the values of A and B would change when the sun casting angle, assigned as α, as shown in Fig.2, changes. The casting angle α is defined as the angle between the sunlight and the plane that contains the aperture line and is vertical to the detector plane (the plane containing the dual triangular detectors). Thus the values of A and B have inherent relations with the casting angle α, which form the principle of operation of the sun sensor. This inherent relationship is the focus of the research in this paper.
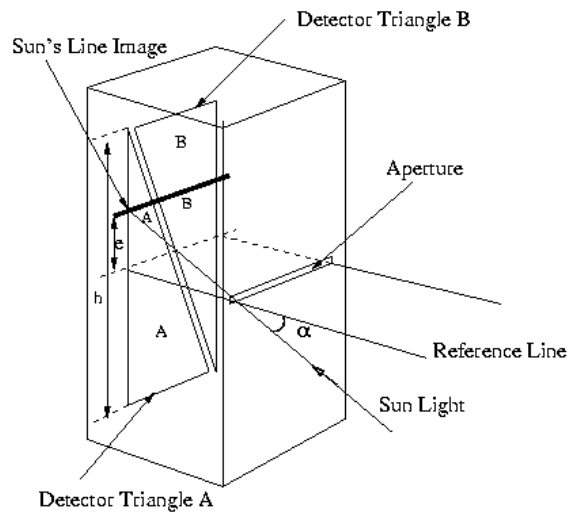
Figure 2 Sun Sensor's Operating Principle

From the geometry, the following relation can be set up,

$$\tan \alpha = \frac{e}{d} = -\frac{h}{2d}\frac{A-B}{A+B} \qquad (1)$$

where d is the focal height between the aperture and the detectors, e represents the distance from the sun's line

2

image to the middle reference line of the detector triangles, and *h* is the total height of the detector triangles.

In the design and manufacturing, the focal height *d* is selected so that at $\alpha = \pm 50°$ the aperture line image is near but not over the endpoints of the detector triangles, the aperture is made sufficiently long such that the off-axis sun angle β, up to $\pm 50°$, still generate an image of the aperture all the way across both triangles. The off-axis sun angle, assigned as β, is defined as the angle between the sun vector and the plane that is vertical to both the aperture line and to the detector plane.

Equation (1) describes the ideal relationship between the sun vector angle α and the sensor's output signal. In practice, however, the sun sensor is subjected to engineering errors coming from different sources. Basically these errors fall into the following categories[5],

- ***Mechanical errors***, coming mainly from manufacturing and misalignments, e.g., inaccuracies in focal height, tilt in the aperture plane, tilt in the detector plane, translation offset of the aperture plane with respect to the detector plane, a rotation of the aperture plane with respect to the detector plane.

- ***Optical and detector errors***, coming mainly from the optical slit and silicon detectors, e.g., imperfection in detector geometry (triangle), imperfection in the photomask aperture geometry, and detector responsivity nonuniformity.

- ***Electrical errors***, coming mainly from the electronic circuits during signal processing, e.g., the nonlinearities in signal amplification, signal distortion due to filtering, as well as errors introduced during analogue/digital (A/D) conversion.

- ***Environmental effects***, as the sensor is exposed to outer space, environmental changes, mainly in radiation and temperature, can influence the sun sensor's measurement accuracy. For example, the detector dark current is a function of both temperature and radiation, increased radiation dose will degrade the responsivity of the detectors, a temperature increase and radiation effects will also increase electronic noise in the output signal.

Among these error sources, the first three sources produce systematic errors, which can be compensated for through systematic ground-based experiments and calibration tests. The environmental effects are non-

systematic errors that need to be calibrated during in-orbit experiments.

To compensate the systematic errors, a ground test experiment is necessary to determine the sun sensor calibration model. Figure 3 illustrates the ground experiment set up as used at SSTL. A Sun emulator is used to produce a strong light beam, a lens is applied to produce collimated light emulating the sun light in space. The sun sensor is fixed to a rotation table, which could produce small accurate rotation angles in azimuth as commanded from a computer. To explore the effects of elevation angles, a small manual rotation device is utilised and mounted between the sun sensor and the rotation table, which allow us to give a tilt angle to the sun sensor in the off-axis direction.

During the experiments, the rotation table is controlled by computer software to rotate by small step increments, and the corresponding output signals are recorded by the computer and saved as a (A-B)/(A+B) ratio directly. Different tilt angles are used to investigate the interference effects from off-axis (elevation) angles. Suppose α and β represent the sun angles of the two orthogonal measurement channels, *x* and *z* represent their corresponding sensor output ration (A-B)/(A+B). Then, for α ratio, β is the off-axis angle. Similarly for β ratio, α become the off-axis angle.

Figure 4 illustrates one set of ground experiment results for an engineering sun sensor, where α is controlled by the rotation table with a step of 1º, and β is manually adjusted with a step of 15º step increment. As seen, for the α axis, the sensor output signal is mainly changing with regards to the angle α, however, the off-axis angle β also influences the sensor output signals. For the β axis, with constant β, the sensor output signal stays approximately the same, however, changes in α do cause small variations to the output signal. Thus cross-coupling effects do exist between the two orthogonal axes.

3. Algebraic Model Analysis

Experimental results revealed that the sun angle is mainly determined by the corresponding sensor output signal. However, cross interferences between the two orthogonal axes do exist, which will limit the measurement accuracy if not considered in the modelling. In other words, α and β should be determined by both *x* and *z* ratios simultaneously to include their mutual cross interferences. To describe this nonlinear muti-variable relationship, a nonlinear algebraic model equation, with a 5th order polynomial

3

relation in the rotation measurement and 2nd order polynomial relation in the tilt (off-axis) measurement, was initially developed and applied to describe this nonlinear relation. It is defined by the following equation,

$$\begin{aligned}
\alpha &= f_\alpha(x,z) \\
&= a_0 + a_1 x + a_2 x^2 + a_3 x^3 + a_4 x^4 + a_5 x^5 + \\
&\quad a_6 z + a_7 zx + a_8 zx^2 + a_9 zx^3 + a_{10} zx^4 + a_{11} zx^5 + \\
&\quad a_{12} z^2 + a_{13} z^2 x + a_{14} z^2 x^2 + a_{15} z^2 x^3 + a_{16} z^2 x^4 + a_{17} z^2 x^5
\end{aligned} \quad (2)$$

$$\begin{aligned}
\beta &= f_\beta(z,x) \\
&= b_0 + b_1 z + b_2 z^2 + b_3 z^3 + b_4 z^4 + b_5 z^5 + \\
&\quad b_6 x + b_7 xz + b_8 xz^2 + b_9 xz^3 + b_{10} xz^4 + b_{11} xz^5 + \\
&\quad b_{12} x^2 + b_{13} x^2 z + b_{14} x^2 z^2 + b_{15} x^2 z^3 + b_{16} x^2 z^4 + b_{17} x^2 z^5
\end{aligned} \quad (3)$$

With this model relation, 18 coefficient parameters are used for each sun sensor axis. To calibrate the model parameters, a least square (LS) estimation algorithm[6] is applied to process the ground experiment data.

For a linear regression model equation,

$$y(t) = \varphi_1(t)\theta_1 + \varphi_2(t)\theta_2 + \Lambda + \varphi_m(t)\theta_m = \varphi(t)^T \theta \quad (4)$$

where $y(t)$ is the observed variable, θ_1, θ_2, Λ, θ_m are unknown parameters, and $\varphi_1, \varphi_2, \Lambda, \varphi_m$ are known functions that may depend on other known variables. Given n test points for the system, i.e., given value $y(1)$, $y(2)$, ... $y(n)$, and $\varphi(1), \varphi(2), \Lambda, \varphi(n)$, the optimal
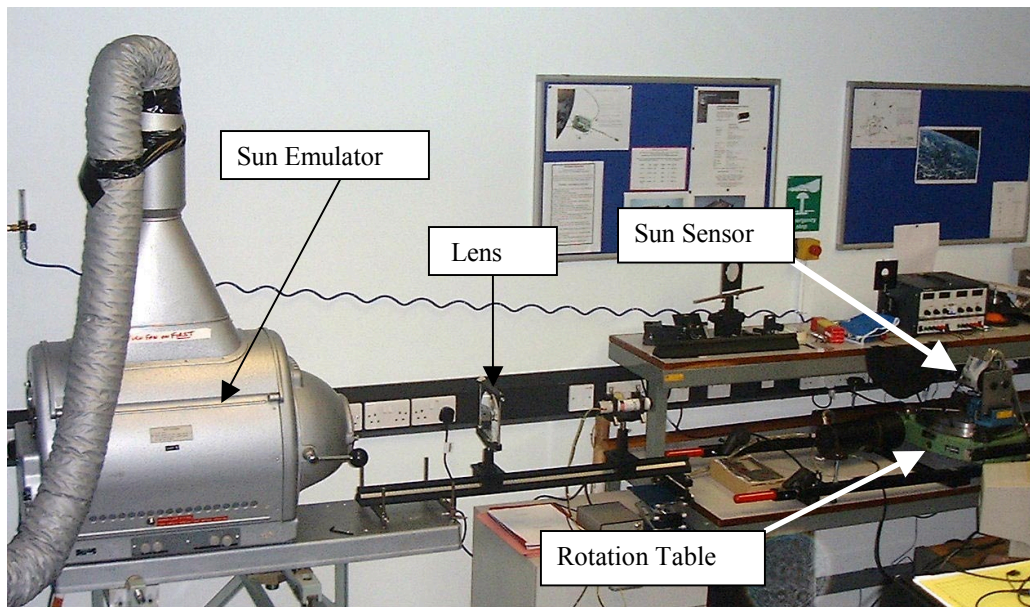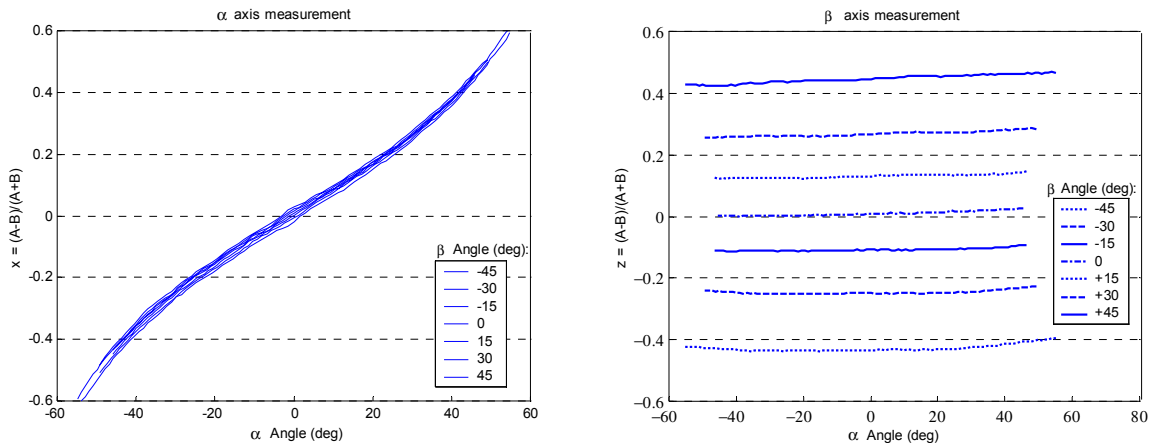

Figure 3 Sun sensor ground test experiments

(a) x- ratio against α and β (b). z-ratio against α and β

Figure 4 Ground experiment results

4

estimation of the model parameters $\hat{\theta}$, which minimize the following least-squares error,

$$V(\theta, n) = \frac{1}{2}\sum_{i=1}^{n} e(i)^2 = \frac{1}{2}\sum_{i=1}^{n}(y(i) - \varphi^T\{i\}\hat{\theta})^2 = \frac{1}{2}E^T E \quad (5)$$

can be determined as[6],

$$\hat{\theta} = (\Phi^T\Phi)^{-1}\Phi^T Y$$
$$= \left(\sum_{i=1}^{n} \varphi(i)\varphi^T(i)\right)^{-1}\left(\sum_{i=1}^{n} \varphi(i)y(i)\right) \quad (6)$$

where: $Y(n) = [y(1) \ y(2) \ y(3) \ \Lambda \ y(n)]^T$

$$E(n) = [e(1) \ e(2) \ e(3) \ \Lambda \ e(n)]^T$$

$$\Phi(n) = \begin{bmatrix} \varphi^T(1) \\ \varphi^T(2) \\ \mathbf{M} \\ \varphi^T(n) \end{bmatrix}$$

With the above LS algorithm, the model parameters in Eq.(2) and (3) can be easily determined from the ground experimental data. Calibration results give a very good accuracy, the corresponding root mean square (RMS) error is 0.219º and average error is 0.167º (see Table 2 for the error definition). Figure 5 illustrates the resulting residual error surface for the rotation angle α (elevation), with respect to the rotation angle α and off-axis angle β (azimuth), corresponding the test results in Fig.4(a).
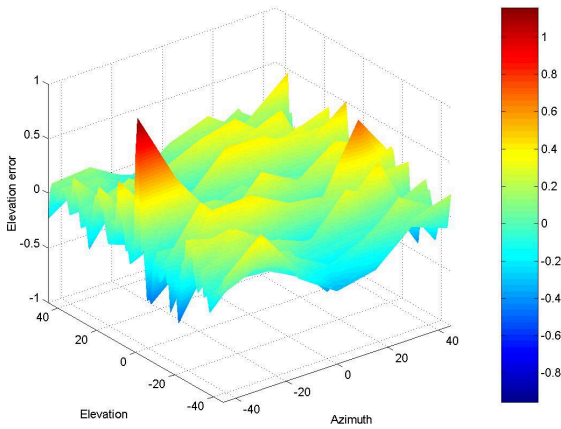

Figure 5 Residual errors with the algebraic model

4. Physical Model Analysis

Although the algebraic model gives a good accuracy from ground calibration tests, it has too many parameters (18 for each axis) with no inherent characteristic or physical meaning. Thus, it will be very difficult to calibrate the model parameters in-orbit, which is required to obtain a satisfactory in-orbit accuracy. For this purpose, a new model is derived in this section, based on physical principles.

4.1 Modelling Analysis

Equation (1) describes the inherent relations between the sun angle and the output signal for an ideal sensor configuration. It can be rewritten as,

$$x = \frac{A - B}{A + B} = -\frac{2d}{h}\tan\alpha = H\tan\alpha \quad (7)$$

where H should be a constant parameter determined by the mechanical configuration of the sun sensor. Figure 4(a) is redrawn as Figure 6. As seen, the basic relation appears to be linear, but the lines are varying due to the off-axis angle interferences.
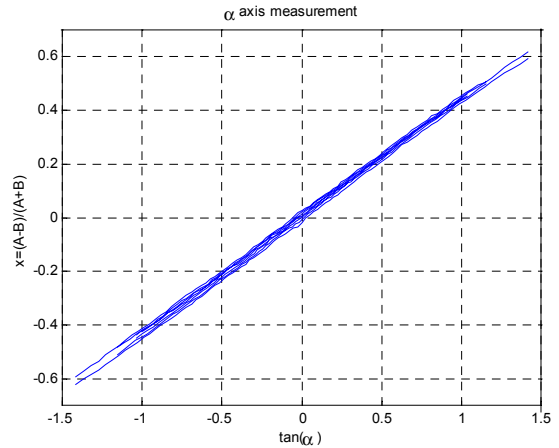

Figure 6 Ground test results

To compensate for the nonlinear systematic errors as discussed in Section 2, a second order relation is introduced,

$$x = H_a \tan^2\alpha + H_b \tan\alpha + H_c \quad (8)$$

To incorporate the cross interferences from the off-axis angle, the coefficients of the linear and constant terms are further modelled as a second-order polynomial relation to the tangent value of the off-axis angle, that is,

$$H_b = H_{b2}\tan^2\beta + H_{b1}\tan\beta + H$$
$$H_c = H_{c2}\tan^2\beta + H_{c1}\tan\beta + H_{c0} \quad (9)$$

Combing Eq(8)-(9), the following model equation is set up,

5

$$x = H_a \tan^2 \alpha + H \tan \alpha + H_{b2} \tan^2 \beta \tan \alpha$$
$$+ H_{b1} \tan\beta \tan \alpha + H_{c2} \tan^2\beta + H_{c1} \tan \beta + H_{c0} \quad (10)$$

The least square estimation algorithm discussed in Section 3 is applied to estimate the 7 model parameters. The resulting residual errors are illustrated in Fig. 7, with a RMS value of 0.317º and an average value of 0.2495º.
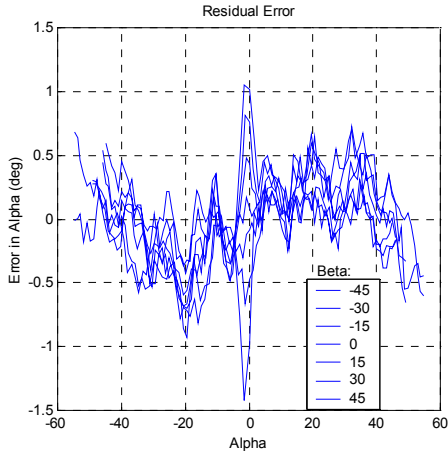
Figure 7 Residual errors in the sun angle with the physical mode (Eq.10)

Analyses on the residual errors for many different test results showed that the errors always have an approximate sine relation to 4α. Thus an additional term is introduced as the eighth parameter to the physical model (Eq.10), which yields,

$$x = H_a \tan^2 \alpha + H \tan \alpha + H_{b2} \tan^2 \beta \tan \alpha$$
$$+ H_{b1} \tan\beta \tan \alpha + H_{c2} \tan^2\beta + H_{c1} \tan \beta \quad (11)$$
$$+ H_{c0} + H_s \sin(4\alpha)$$

With this model equation, the resulting residual errors are illustrated in Figure 8, with an RMS value of 0.247º and an average value of 0.1875º.

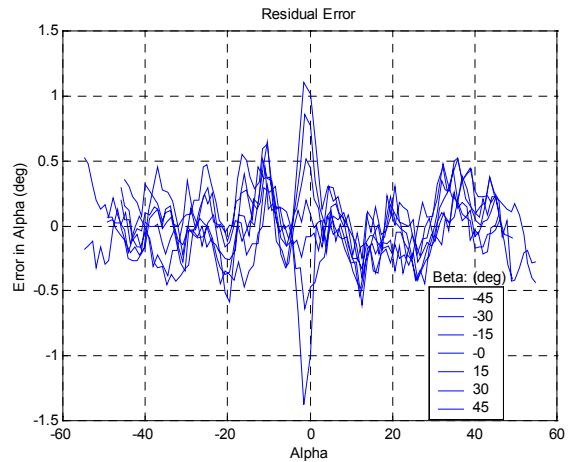**4.2 Parameter Sensitivity Analyses**

The new physical model gives a similar calibration accuracy for the sun angles to be measured from the sensor output ratios. However, it has much less parameters, 8 compared to 18 in the algebraic model. Furthermore, the role and importance of each parameter are better defined. For the purpose of in-orbit calibration, it will be important to have a good understanding of the role and importance of each parameter in the model equation.

For this purpose, a sensitivity analysis was done for the new physical model, with a complete set of ground

experimental data. Based on the optimal estimated value of each parameter obtained from the LS algorithm, a small amount of change, e.g. 10%, is added to each parameter. This new parameter value is applied to the model equation to check how the errors change. The sensitivity of this parameter is defined as the ration of the changes in the RMS value of the residual errors over that of the parameter, i.e.,

$$sensitivity = \frac{\Delta Err}{\Delta H_i} \quad (12)$$

where *Err* is the RMS value of the residual errors, H_i is the model parameter, Δ represents the changing amount of the corresponding argument.

Figure 8 Residual errors in the sun angle with the physical model (Eq.11)

For a specific set of ground tests results, the sensitivity analysis for the eight parameters is illustrated in Table 2.

Table 2 Summary of the model parameter sensitivities

Parameter	Optimal Value	Sensitivity	Importance
H_a	-0.001523	1.95	*
H	0.4361	33.2	***
H_{b2}	-0.001338	10.08	**
H_{b1}	-0.003826	2.12	*
H_{c2}	-0.003218	4.74	*
H_{c1}	0.01680	10.06	**
H_{c0}	0.007376	31.29	***
H_s	0.004115	12.44	**

6

The role and importance of each model parameter can be summarized as follows,

- H_a is mainly to compensate for nonlinear factors of the sensor measurements, especially at large angles. Calibration shows this parameter is very small, and its influence on the modelling accuracy is also very small.

- H is the most important parameter in the model equation. It defines the major relation between the measurements and the tangent values of the angles. Sensitivity analysis results supported this point, as illustrated in Table 2.

- H_{b2} is an important parameter to take account of the cross interference from the off-axis angle β. It has big influence on the modelling accuracy. Test results in Table 2 prove this point. Its value determines the slope of the test line (similar to parameter H) for off-axis angles.

- H_{b1} is another parameter to calibrate for the cross interference from the off-axis angle. It mainly compensates for the unsymmetrical character of the cross interference between positive and negative β angles. Its value should be very small if the sensor has good symmetric properties, as shown by the results in Table 2. Its influence to the modelling error is also very limited.

- H_{c2} calibrates the slight changes caused by cross interferences to the sensor output signal. Using second order curve fit for cross-interference, which results the parameter H_{c2}, is to enhance the accuracy and take account for nonlinear factors. Its role is not important, as illustrated in Table 2.

- H_{c1} calibrates also for slight changes caused by cross interferences to the sensor output signal. It compensates for the unsymmetrical character in the sensor output with respect to positive and negative off-axis angles. In engineering, there are always errors in manufacturing and assembling, though they may be very small. Thus, this parameter plays an appropriate role in the modelling accuracy, as illustrated in Table 2.

- H_{c0} plays a very important role in compensating for the initial off-set between the aperture line and the middle reference line of the double triangle detector. It actually causes a slight shifting of the sensor's output line to pass through the zero point at the zero sun angle, as shown in Fig. 6. Additionally, the position errors caused by mechanical alignment of the sensor to the satellite body can also be compensated for by this parameter.

- H_s plays an appropriate role to compensate the residual errors. Its physical meaning is not yet clear. However, it contributes to a further enhancement in the modelling accuracy.

The importance of each parameter to the modelling accuracy is further explored by fixing some parameters to zero (i.e., to remove some terms) in the physical model. The resulting errors for the same ground test data are summarized in Table 3, which gives a clear understanding of each parameter's importance in the model equation. As seen, the most important parameters in the model equation should be H, H_{c0} and H_{c1}. Each of the other parameter contribute to some improvement of the accuracy, as shown in Table 3.

Table 3 Modelling performance for different parameter combination

No. of Para.	Description	E_{avg} * (deg)	E_{RMS} ** (deg)
8	Complete model equation	0.1875	0.2470
7	$H_s = 0$;	0.2495	0.3173
6	$H_s = 0$, $H_a = 0$	0.2531	0.3205
5	$H_s = 0$, $H_a = 0$, $H_{b1} = 0$	0.2478	0.3502
4	$H_s = 0$, $H_a = 0$, $H_{b1} = 0$, $H_{c2} = 0$	0.2938	0.3737
3	$H \neq 0$, $H_{c0} \neq 0$, $H_{c1} \neq 0$	0.2980	0.3796
3	$H \neq 0$, $H_{c0} \neq 0$, $H_{b2} \neq 0$	0.9221	1.1602
2	$H \neq 0$, $H_{c0} \neq 0$	0.9286	1.1607
1	$H \neq 0$	1.0908	1.3099

$$^* E_{avg} = \frac{1}{n} \sum_{i=1}^{n} |e_i|, \quad ^{**} E_{RMS} = \sqrt{\frac{1}{n} \sum_{i=1}^{n} e_i^2}$$

4.3 Computation Algorithms

The new physical model (Eq. 11) has mixed the two angles together. Thus it is impossible to solve for the sun angles directly from the two sensor outputs, x and z. An iterative approach must be used to compute the angles to be measured. First, the following simplest linear relation without cross interferences can be used to get the initial estimation for α,

$$x = H \tan \alpha + H_{c0} \qquad (13)$$

7

Then an iteration process based on the following equation can be used to refine the angles, until they converge to a required accuracy.

$$\alpha_{i+1} = \tan^{-1} \left\{ \frac{x - (H_{c2} \tan^2 \beta_i + H_{c1} \tan \beta_i + H_{c0}) - H_s \sin(4\alpha_i)}{H + H_a \tan \alpha_i + H_{b2} \tan^2 \beta_i + H_{b1} \tan \beta_i} \right\}$$

(14)

where the subscript i represents the ith estimation value.

Another approach for on-board application is to use other available sensors, such as a horizon sensor or magnetometer, to determine the initial estimation of the sun angles, then to start the iteration process to solve the model equations.

5. In-Orbit Calibration

The ground calibration tests and analyses can significantly reduce the systematic mechanical, optical and electrical errors. However, after putting the satellite into orbit, the performance of the sun sensor would degrade with radiation and with temperature, as well as possible mechanical misalignment during the launch. The primary environmental effects can be catalogued as follows[5]:

- Increase in detector dark current as a function of both temperature and radiation,

- Physical distortion of the module due to changes in temperature and mismatches in material CTE (coefficient of thermal expansion)

- Nonuniform degradation of the responsivity of detector A and B with increasing radiation

- Increases in electronic noise over both temperature and radiation.

Thus to get a higher performance, in-orbit calibration is further required to compensate for the potential errors introduced by the launching process and space environmental changes.

For the sun sensors on-board UoSAT-12, the ground-based calibration experiments were not properly done for the cross interferences between the two axes, due to a lack of understanding about the cross interferences. Only simple tests along one axis were done before the launch. For the sun sensors on-board Tsinghua-1, the ground test results were not very reliable due to the lack of a proper Solar emulator and related test equipments. Thus in-orbit calibration tests for the sun sensors on-board these satellites became necessary to obtain an improved accuracy.

The biggest difficulty for in-orbit calibration is the lack of accurate information of the real sun angles during flight. However, as is normal, there are always other alternative sensors to help determine the satellite's attitude. For UoSAT-12, magnetometers and horizon sensors were used. For Tsinghua-1, only a magnetometer is available to determine the satellite's attitude approximately. In other words, alternative satellite attitude information is available from the on-board Kalman filter. Satellite orbital position can be calculated from the Norad two-line-element data based on the SGP4 orbital propagator[7]. With this information, in-orbit calibration of the sun sensors on-board UoSAT-12 and Tsinghua-1 were conducted, with the principle illustrated in Figure 9. The Sun sensor's output signals (x and z) and the available attitude information from the ADCS (attitude determination and control system) on-board filter (OBF), sampled every ten second, were downloaded using a log-file. By using the time information from the log-file and the NORAD data, the position vectors of the satellite and Sun can be easily computed, thus the unit direction vector of the Sun to the satellite can be determined and transformed into the orbital coordinate frame[2]. The downloaded attitude information is used to transform this direction vector into the satellite body coordinate frame[2]. Then the reference sun angles (α and β) are available. Together with the downloaded sun sensor's output signals, the least square estimation algorithms can be used to calibrate the model parameters.
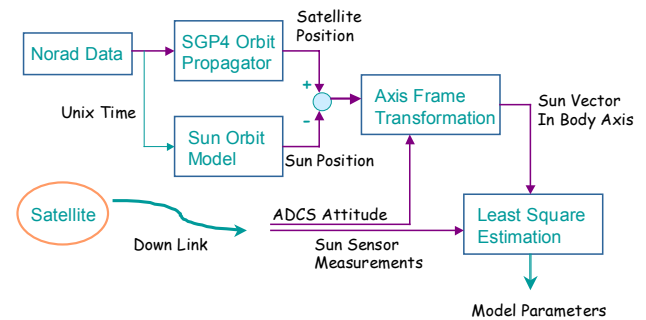

Figure 9 In-Orbit Calibration Principle

The in-orbit data are downloaded once per day. As the sun vector varies over a small range during an orbit with respect to a sun sensor, the calibration data should be gathered for many different days to cover a large enough working envelope of the sun sensor. To proceed with different days, the algorithm of Eq.(6) are used for all days in an sequential way for each sensor axis, as described in the following.

For every day, the in-orbit data are processed to determine how many test points are available for a

8

specific sun sensor, then these valid points are processed as following,

$$P_k = \sum_{i=1}^{n_k} \varphi(i)\varphi^T(i) \qquad (14)$$

$$Z_k = \sum_{i=1}^{n_k} \varphi(i)y(i) \qquad (15)$$

where k represent the day number, n_k represents the available test points on the kth day for a specific sun sensor.

Then starting with the first day's results, the model parameters can be estimated approximately as,

$$\hat{\theta}_1 = (P_1)^{-1} Z_1 \qquad (16)$$

As more data becomes available for other days, the parameters are updated in the following way,

$$\hat{\theta}_k = \left(\sum_{j=1}^{k} P_k\right)^{-1} \left(\sum_{j=1}^{k} Z_k\right) \qquad (17)$$

Thus, as more data for the successive days become available, the parameters are recalibrated with the new test results.

With the above sequential LS algorithms, the available in-orbit data from UoSAT-12 sun sensor for 24 days, downloaded in the period March to May 2000, are used to calibrate the model parameters of the four on-board sun sensors. Figure 10 shows the convergence process of the two most important model parameters of all eight axes. As seen, the parameter H converges to its final value of around 0.41, the difference in the sign is caused by the polarity definition (A and B) for the elevation and azimuth axis. All eight axes converge to the same value, which means that the four sun sensors were manufactured consistently. The parameter H_{c0} also converges to steadily their specific values. The differences in their steady state values amongst the eight axes demonstrate the differences in errors caused by position off-set within the sensor and installation misalignment to the satellite. Calibration results for the other parameters are available from an internal technical note[8].

By applying the in-orbit calibration results back to the in-orbit application, great improvements in satellite attitude determination were observed. Figure 11 illustrates the tracking performances of sun sensor No.2 on-board UoSAT-12, before and after the calibration. The x-axis is the sampling numbers when the sun sensor is active, the y-axis is the tracking error between the

sun's reference angle and the estimated value from the sun sensor's output signals, on the sun vector's elevation (EL) and azimuth (AZ) angles in the body reference frame. As seen, great improvements were achieved through the above in-orbit calibration analyses. Similar in-orbit calibration analyses were also done for the Tsinghua-1 satellite. As Tsinghua-1 satellite has only a magnetometer to determine the reference sun angles, the accuracy of the available reference angles were not very good, therefore, the final performance for Tsinghua-1 satellite is not as good as that for UoSAT-12. Table 4 summarizes the final performance improvements for these two satellites.
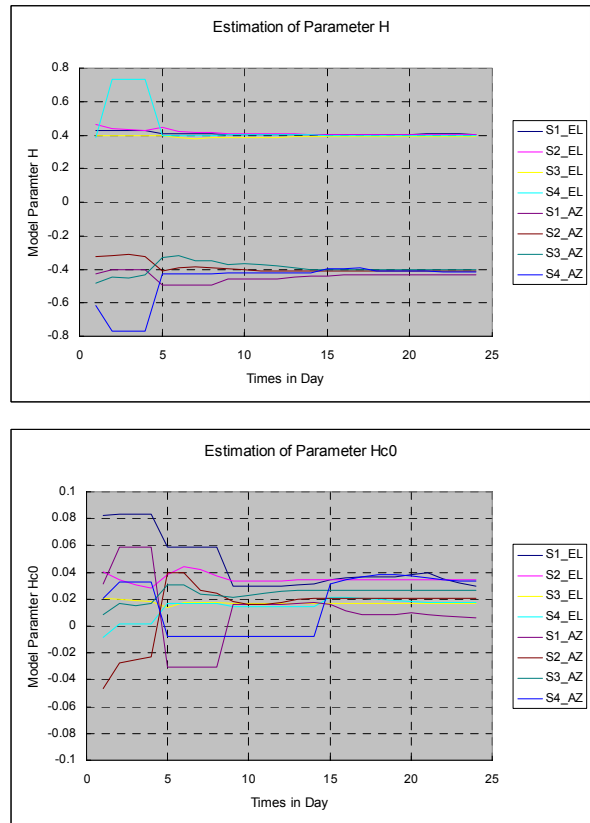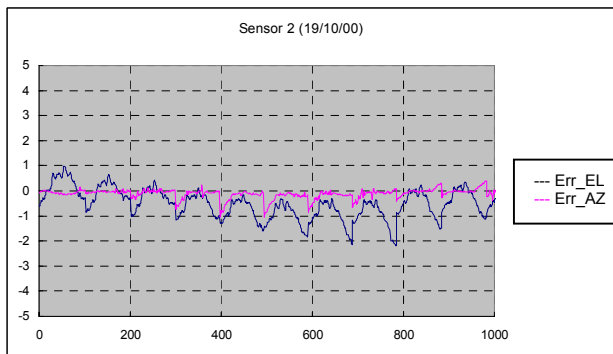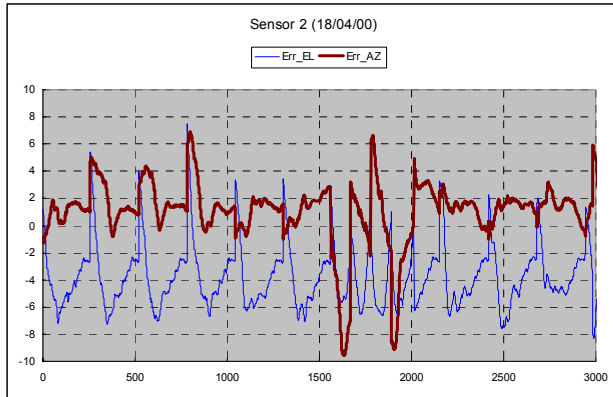

Figure 10 In-Orbit calibration process of the model parameters

The above calibration approach is very flexible in that the user has the freedom to calibrate only certain of the 8 parameters, while using the ground-based results for other parameters. For example, the less important parameters, such as H_a, H_{b1}, H_{c2}, H_s, can be fixed to the available ground-based calibration results, while the other 4 parameters can be recalibrated using in-orbit data. The in-orbit calibration for Tsinghua-1 sun sensors was done in this way.

9

Table 4 Performance improvements with in-orbit calibration

	UoSAT-12		Tsinghua-1	
	Max Err	Average Err	Max Err	Average Err
Before Calibration	< 8 deg	< 1.0 deg	< 10 deg	< 2.0 deg
After Calibration	< 2 deg	< 0.1 deg	< 3 deg	< 0.5 deg

Figure 11 Sun Sensor angle errors before and after the in-orbit calibration

6. Conclusion

In this paper, the modelling relations and calibration techniques of the analogue miniature sun sensors manufactured at SSTL were discussed. The major points can be summarized as following.

1) Two model equations have been developed to describe the sun sensor's internal calibration. The algebraic model is developed based on polynomial curve-fitting, while the physical model is developed based on theoretical analyses and the physical geometry of the sun sensor. Auxiliary terms are added into the physical model equation to compensate for various nonlinear errors. This model has the following advantages over the algebraic model equation, though for the same ground test data they give a similar modelling accuracy:

- The number of parameters has been reduced from 18 to 8, which makes it easier to analyse and calibrate.

- Each parameter has direct physical meaning and its role and effect in the model equation is better understood. Thus it is easier to interpret during calibration analyses, especially for in-orbit applications.

- Aids the sensitivity analyses, which reveal the importance and contribution of each parameter to the modelling accuracy.

2) A sensitivity analysis is presented for the physical model parameters based on the available ground test data. The results give a better understanding of the importance of each model parameter.

3) An in-orbit calibration approach has been proposed and used for the sun sensors on-board UoSAT-12 and Tsinghua-1, based on the available information. The available estimated attitude information are used to transfer the sun vector from the orbital frame to the satellite body frame, thus producing the reference angles for the sun sensor's output.

4) A sequential (not recursive) least square estimation algorithm has been developed to handle the numerous in-orbit test data in a sequential way, based on the principle of least-square estimation. It handles the in-orbit data of one day in a batch filter, while different day's test-data can be processed in a sequential way. As more data becomes available, the model parameters are further improved, while the previous test data in kept at an equal weighting. Practical test results from the in-orbit test data revealed that this algorithm gives improved estimation results for the model parameters. As more in-orbit data becomes available, further improvements can be expected.

The research results supported the following conclusions,

- Both model equations proposed in this paper can accurately fit the sun sensor measurement relations, while the physical model is more feasible for calibration analyses.

10

- The in-orbit calibration approach presented in this paper is feasible to be implemented in practice.

- The sequential least square estimation algorithm works properly during in-orbit calibration of the sun sensor model parameters.

- The principles and methods presented here can also be used for other attitude sensor's calibration analyses.

References

[1] Kouzmin, V.S., Cheremoukhin, G.S., and Fedoseev, V.I. "Miniature Sun Sensor", Proceedings – SPIE the International Society for Optical Engineering (ISSN: 0361-0748), Issue 2739, pp407-410, 1996.

[2] Wertz, J.R. (ed.) "Spacecraft Attitude Determination and Control", D. Reidel Publishing Company, Dordrecht, The Netherlands, 1985.

[3] Zabiyakin, A.S., Prasolov, V.O., Baklanov, A.I., Eltsov, A.V., and Shalnev, O.V., "Sun Sensor for Orientation and Navigation Systems of Spacecraft", Proceedings – SPIE the International Society for Optical Engineering, Issue 3901, pp106-111, 1999.

[4] Doll, B., Pitz, W., Duschl, I. And Settelmeyer, E. "A New Technology Coarse Earth & Sun Sensor", Proceedings of the International Symposium on Space Technology and Science, Vol 21st/1, pp1039-1041, AGNE Shofu Publishing Inc., Japan.

[5] Zaffanella, C. and McGorty, C. "Miniature Analog Sun Sensors – A Unique Building Block Approach", Advances in the Astronautics Sciences, Vol 92, 1996, pp439-451.

[6] Astrom, K.J. and Wittenmark, B. "Adaptive Control", Addison-Wesley, Massachusetts, 1989.

[7] Hoots, F.R. & Roehrich, R.L. "Models for Propagation of NORAD Element Sets", SPACETRACK REPORT NO. 3, Aerospace Defence Centre, Peterson, USA.

[8] Wu, S-F. "In-Orbit Calibration Analysis of the Sun Sensors on-board UoSAT-12", Technical Report, Surrey Space Center, University of Surrey, July, 2000.

11